Crystal detector background of the SABRE South experiment

Guangyong Fu on behalf of the SABRE South Collaboration
The University of Melbourne
guangyongf@student.unimelb.edu.au

TIPP 2023 @ CAPE TOWN

Dark matter modulation

DAMA reports a dark matter annual modulation signal at 13.7σ confidence level in (2-6) keV

- Amplitude : (0.01014 ± 0.00074) cpd/kg/keV
- Period: (0.99834 ± 0.00067) yr
- phase: (142.4 ± 4.2) days

$$S(t) = B + S_0 + S_m \cos(\omega(t - t_0))$$

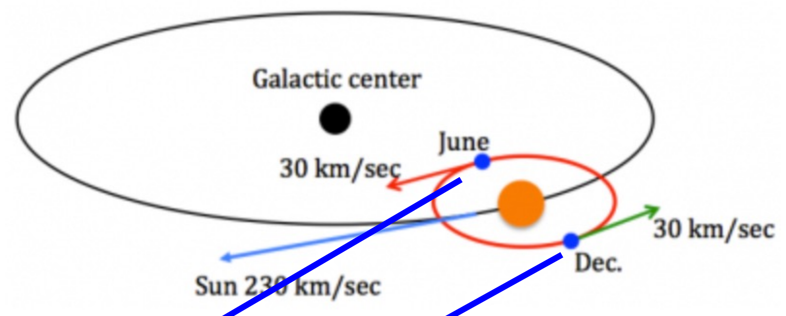

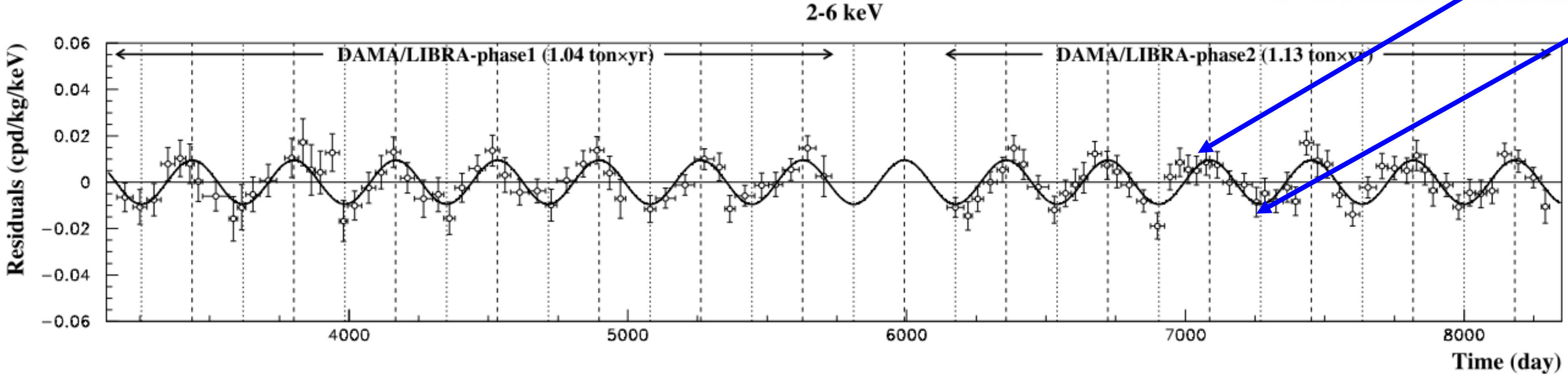

DAMA Collaboration. Nucl. Phys. At. Energy 22 (2021) 329-342

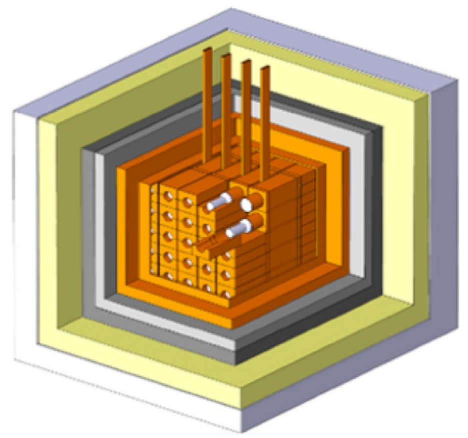

DAMA/LIBRA set-up

Dark matter modulation

- WIMPs (Weakly interacting massive particles) interact with matter through nuclear recoil
- Clear modulation is presented below 6 keV
- COSINE-100, ANAIS have not confirmed or rejected DAMA's modulation signal. (See Karoline Schaeffner's talk @ Plenary Session 2)

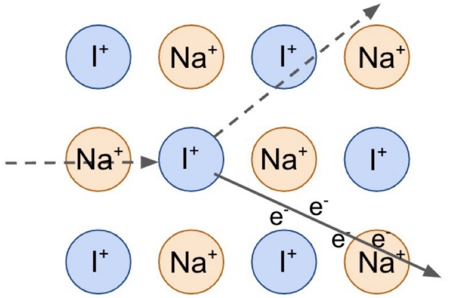

DAMA's modulation signal remains unresolved

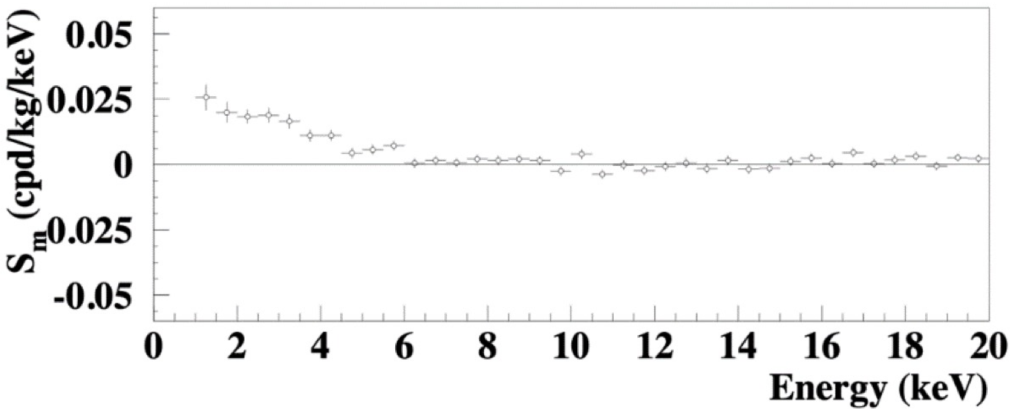

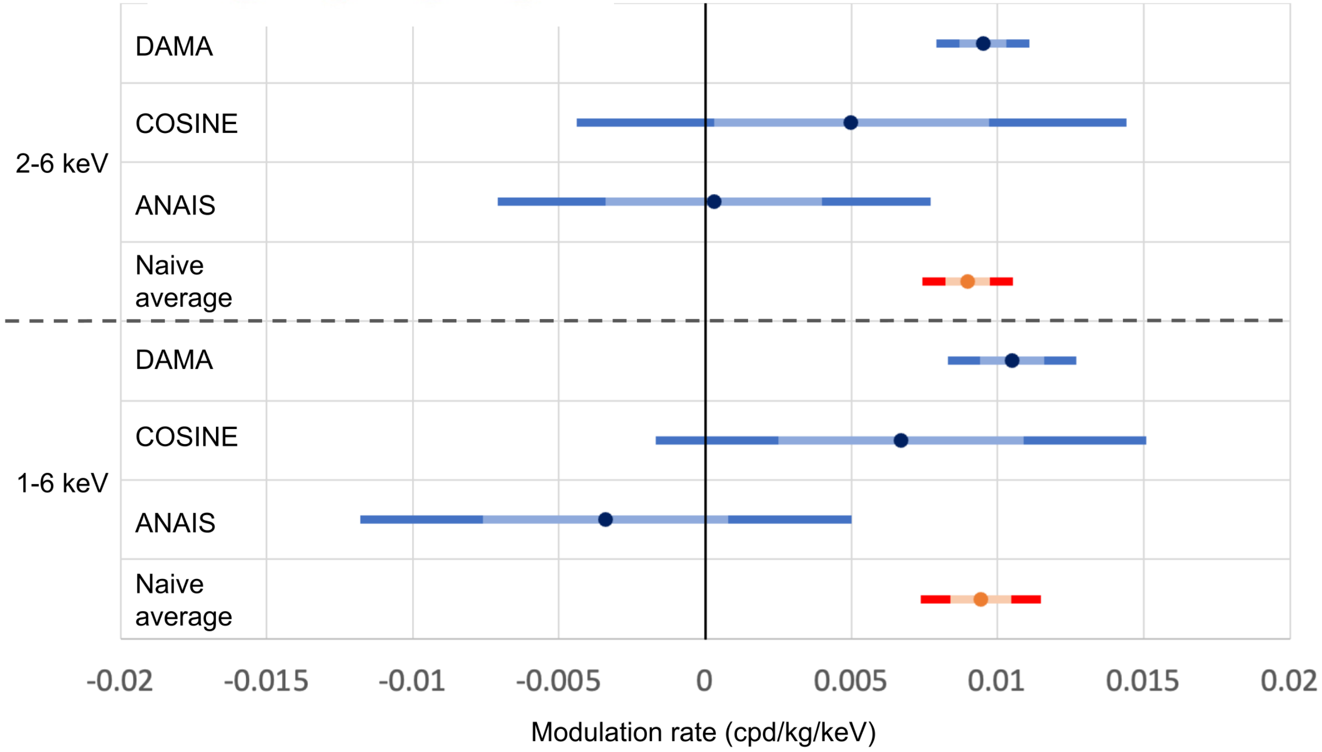

[1] DAMA Collaboration. Nucl. Phys. At. Energy 22 (2021) 329-342

[2] COSINE-100. *PRD* 106.5 (2022): 052005.

[3] ANAIS. *Physical Review D* 103.10 (2021): 102005.

SABRE: a dual site experiment

ARC CENTRE OF EXCELLENCE FOR DARK MATTER

THE UNIVERSITY OF MELBOURNE

The ambitious program of SABRE foresees two detectors in both hemispheres to disentangle seasonal or site-related effects from the dark matter-like modulated signal

- SABRE North at Laboratori Nazionali del Gran Sasso (LNGS) in Italy
- SABRE South at Stawell Underground Physics Laboratory (SUPL) in Australia

SAPIENZA UNIVERSITÀ DI ROMA

PRINCETON UNIVERSITY

UNIVERSITÀ DEGLI STUDI DI MILANO

UNIVERSITÀ DEL SALENTO

INFN LNGS
Istituto Nazionale di Fisica Nucleare
Laboratori Nazionali del Gran Sasso

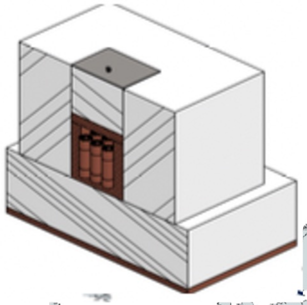

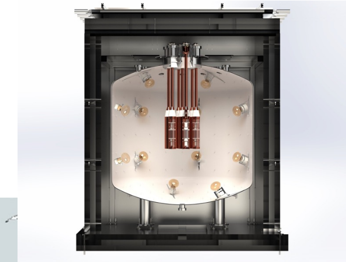

STAWELL UNDERGROUND PHYSICS LAB

KEK

ARC CENTRE OF EXCELLENCE FOR DARK MATTER PARTICLE PHYSICS

THE UNIVERSITY of ADELAIDE

THE UNIVERSITY OF MELBOURNE

SWINBURNE UNIVERSITY OF TECHNOLOGY

Australian National University

THE UNIVERSITY OF SYDNEY

SUPL

- Stawell Underground Physics Laboratory (SUPL) is the first underground laboratory in the Southern Hemisphere,
- 1025 m underground,
- Muon flux will be attenuated to 10^{-6} of the surface,
- Construction completed in 2022/2023, and detector to be assembled in 2023-2024.

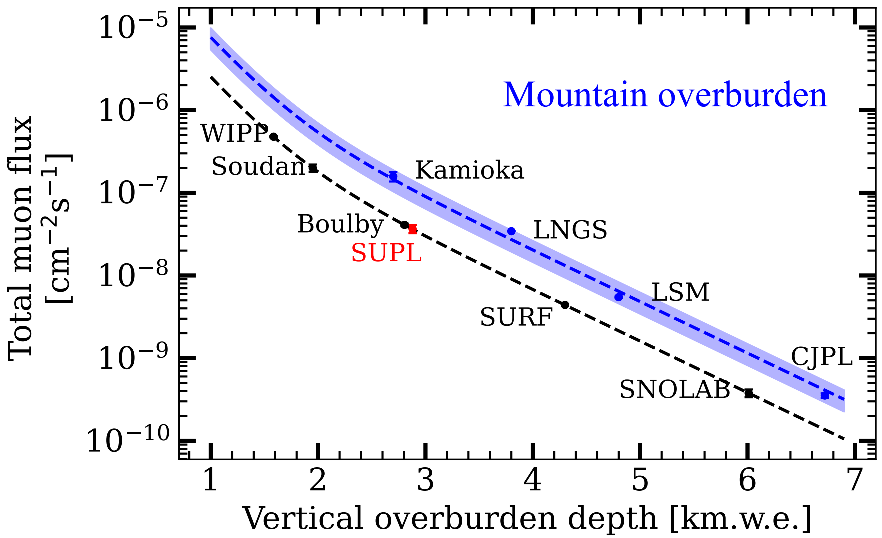

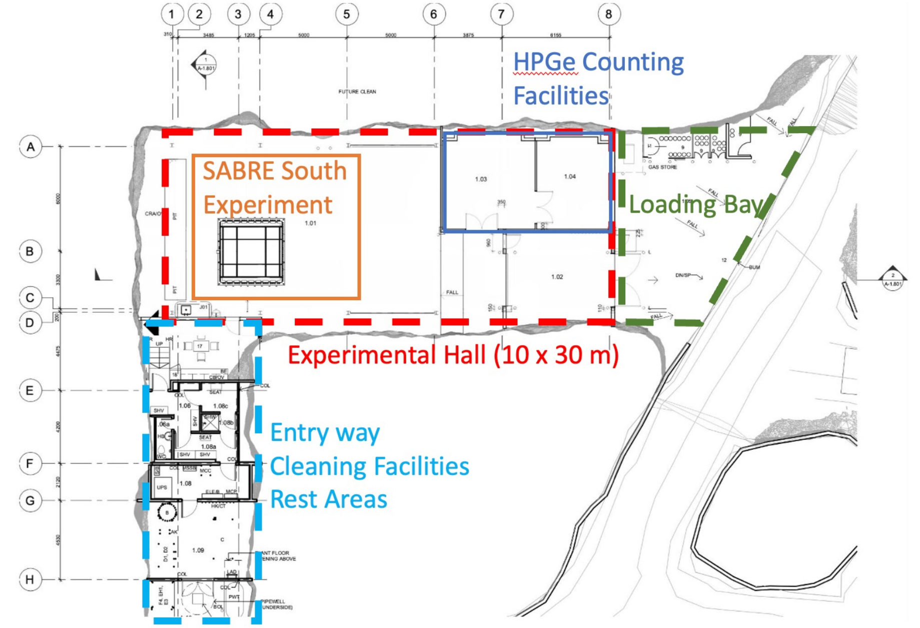

SABRE South detector

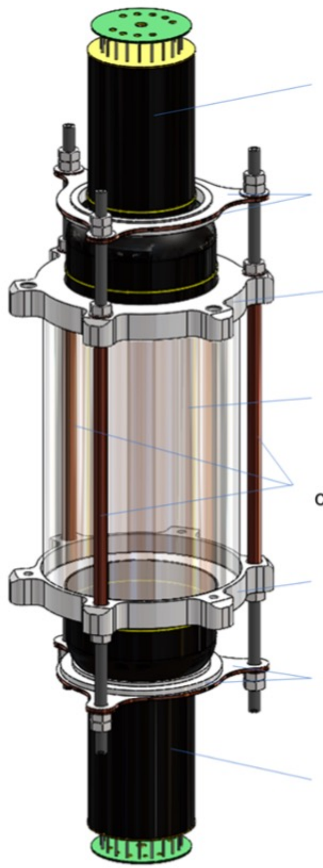

Details on the SABRE South trigger and data acquisition systems see Lachlan McKie's talk @ A3.

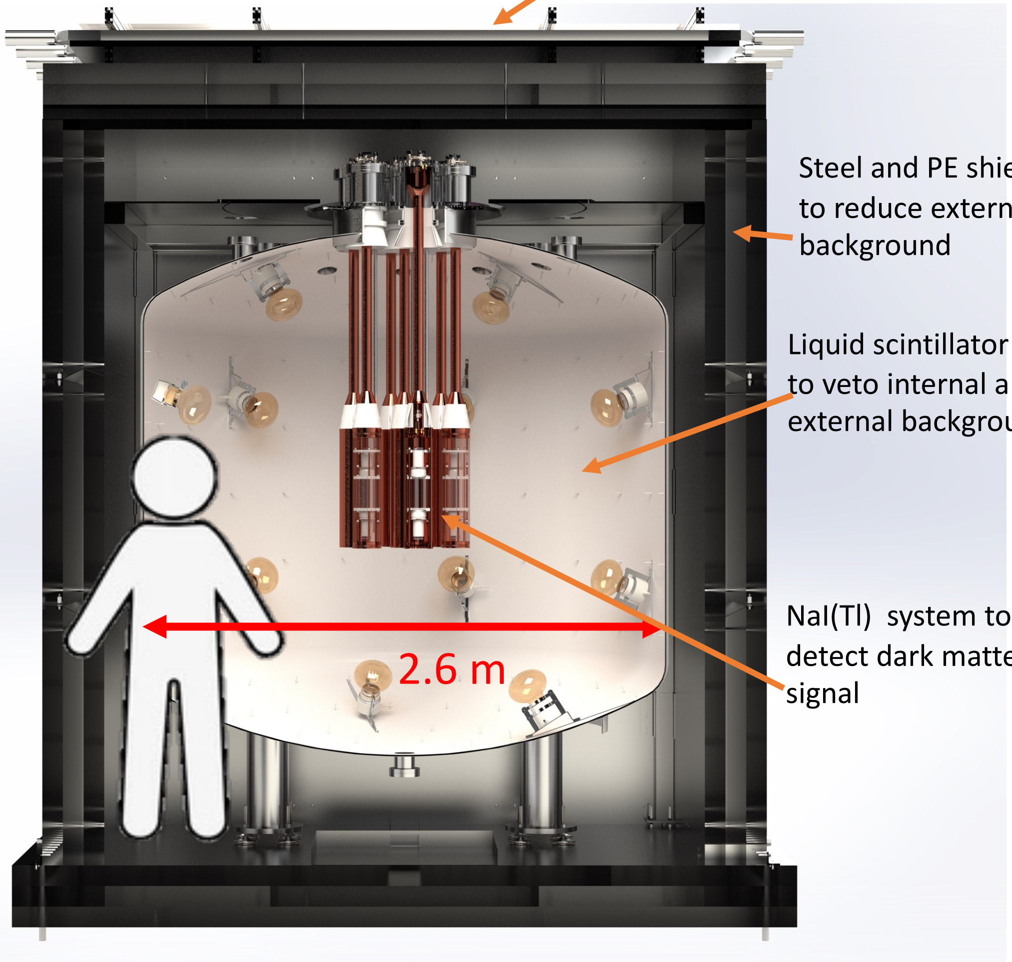

SABRE South detector components

Component	Specifications
NaI(Tl) system	
NaI(Tl) crystals	7 × 5-7 kg - length ∼15-20 cm, dia. ∼10 cm
R11065 Hamamatsu PMTs	2 per crystal, 76.2 mm dia.
Oxygen free high thermal conductivity Copper enclosure	1 per crystal
Teflon holder	1 per crystal
Feedthrough plate	1 per crystal
Copper conduit	1 per crystal, 84 cm in length
Aluminium calibration tubes	3 of length 1.5 m
CAEN V1730 digitiser	500 Ms/s sample rate
Liquid scintillator system	
Linear alkylbezene (LAB)	11,600 litres
PPO	∼3.5 g/L
Bis-MSB	∼15 mg/L
R5912 Hamamatsu PMTs	3 (top) + 12 (sides) + 3 (bottom), 204 mm dia.
Stainless steel vessel	3 m (height) × 2.6 m (diameter)
Lumirror coating	Internal wrapping of vessel
CAEN V1730 digitiser	500 million samples/s sample rate
Shielding	
Carbon steel	2 layers of 80 mm thickness for total mass of 105 tonnes
Polyethlyene	1 layer of 100 mm thickness for a total mass of 6.6 tonnes
Rock overburdern	1025 m (2900 m water equivalent)
Muon system	
EJ200 with double sided fishtail light guides	8 modules 300 cm × 40 cm × 5 cm
R13089 Hamamatsu PMTs	2 per module
CAEN V1743 digitiser	3.2 billion samples/s sample rate

Crystal production

A number of crystals have been grown by Radiation Monitoring Devices (RMD).

- The crystals are grown from Merck Astrograde NaI powder, with potassium contamination < 10 ppb.
- Bridgman-Stockbarger method is used to prevent additional contamination introduced during the growth process.
- Impurities measured with inductively coupled plasma mass spectroscopy (ICP-MS)

Ongoing collaboration with SICCAS to produce high-purity crystals.

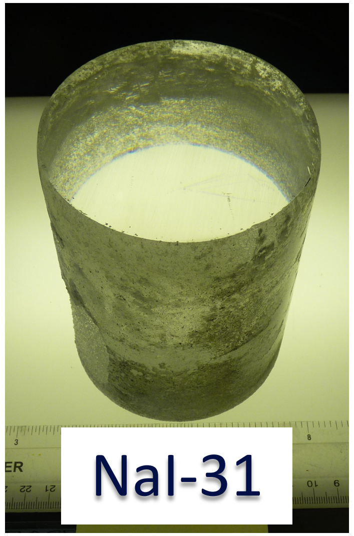

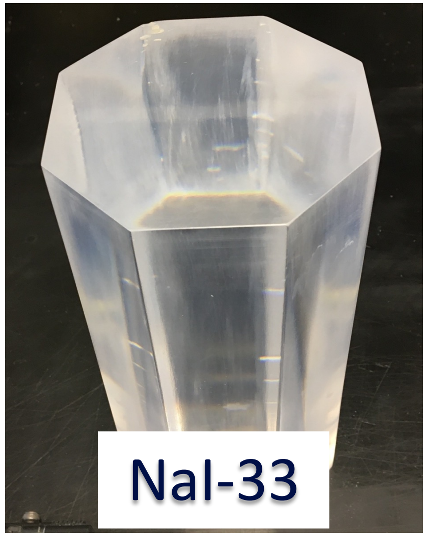

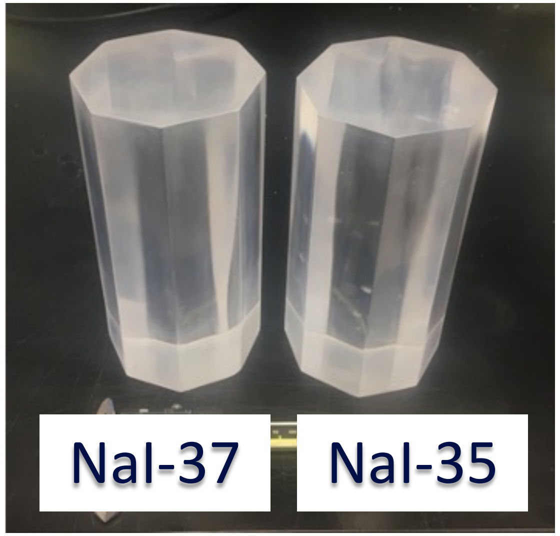

Crystals	Mass [kg]	LY [pe/keV]	^{39}K [ppb]	^{238}U [ppb]	^{232}Th [ppb]	Rate (1-6 keV) [cpd/kg/keV]	Exposure [kg day]
NaI - 31	3.00	9.1±0.1	16.5±1.1	-	-	2.74±0.03	786
NaI - 33 [a]	3.40	11.1±0.2	4.3±0.8	0.47±0.05	0.40±0.07	0.95±0.05	95.2
NaI - 35	4.36	8.7±0.1	8.3±0.6	0.18±0.03	-	1.26±0.35 [b]	35.6
NaI - 37	4.35	7.8±0.2	8.0±0.6	0.61±0.05	0.27±0.06	2.71±0.05 [b]	243.6

a: SABRE PoPl-dry in new shielding
b: Preliminary rate in [2,6] keV ROI

[1] B. Suerfu PhD thesis, Department of Physics, Princeton University, 2018.

Crystal measurements

NaI-33 measurements:

- Light yield measured with ^{241}Am 59.5 keV gammas to be 11.1 ± 0.2 phe/keV, energy resolution is 13.2% (FWHM/E).
- ^{40}K, ^{210}Pb, ^{129}I from spectral analysis.
  - Activities treated as free or semifree parameters: ^{40}K, ^{210}Pb, ^{3}H, ^{226}Ra, ^{232}Th, ^{129}I, ^{121m}Te, ^{127m}Te,
  - Constrained by ICP-MS measurements of ^{40}K from crystal off-cuts, upper limits of ^{87}Rb, ^{238}U and ^{232}Th in the crystal powder, and ^{210}Pb by alpha counting
  - A flat component includes ^{87}Rb and other internal and external background contributions.

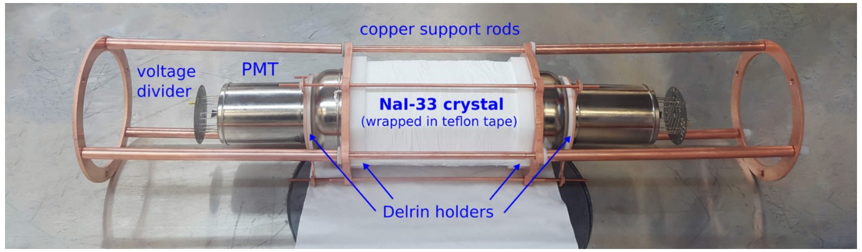

NaI-33 calibration with ^{241}Am source

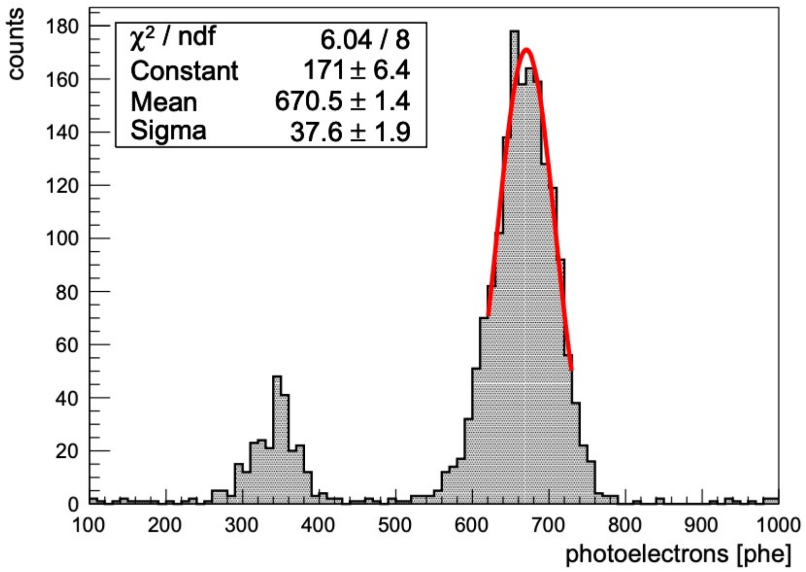

Energy spectrum from NaI-33 in 0-100 keV with a spectral fit

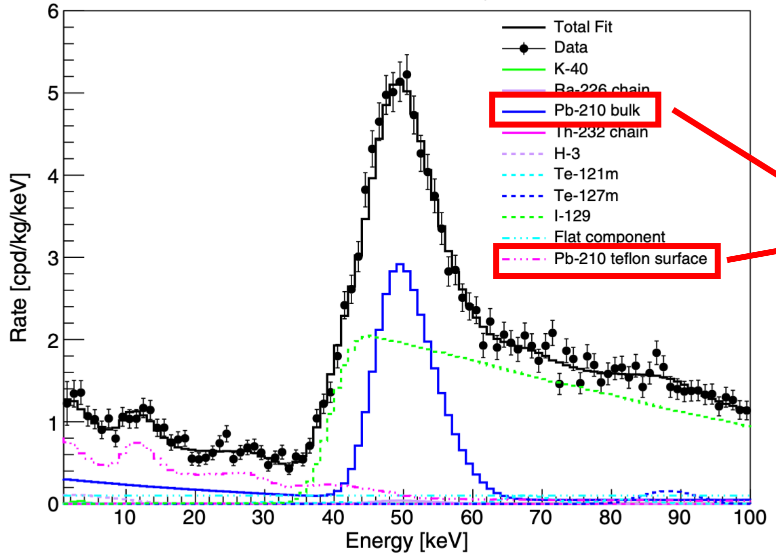

Dominate in ROI (1-6 keV)

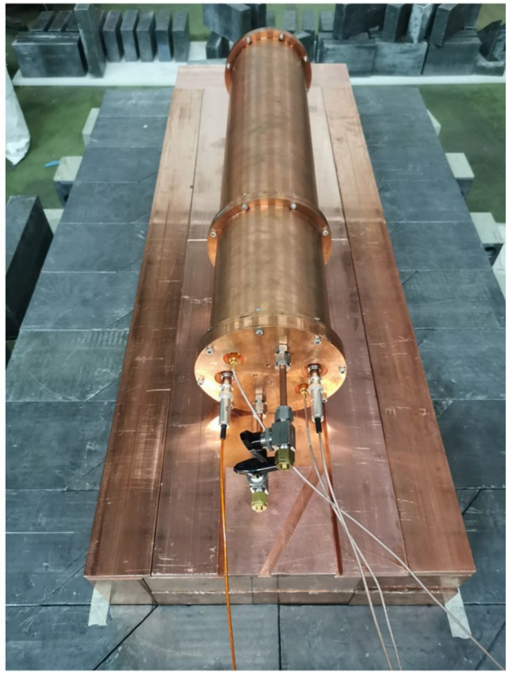

[1] SABRE, EPJC 81(4) (2021).
[2] SABRE, PHYS. REV D 104, L021302 (2021)

Zone refining

Working with SABRE North, RMD, Princeton University, MELLEN to use zone refining to further purify ultrahigh-purity NaI powder

- A zone is melted and moved across the ingot in the same direction.
- As the zone is moved, newly formed crystal has less impurities than the molten liquid.
- This process is repeated multiple times so that the impurities are pushed towards the end.
- Suitable for ~ 100 kg powder
- Th doping after zone refining

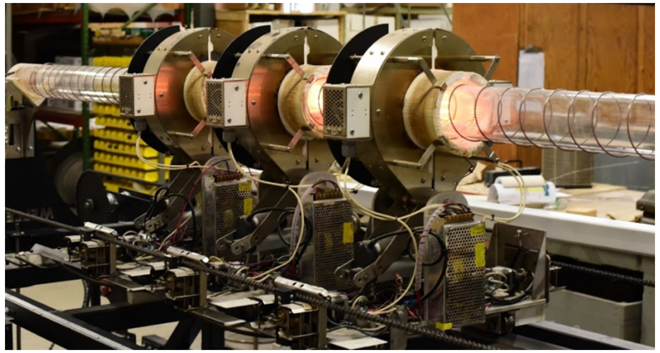

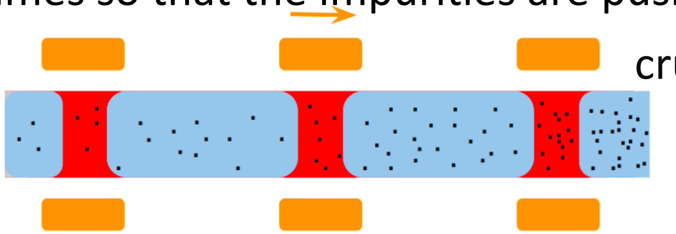

Isotope	Impurity concentration (ppb)					
	Sample location (mm)					
	Powder	7 ± 7	325 ± 9	492 ± 10	635 ± 20	783 ± 30
^{39}K	7.5	< 0.8	< 0.8	1.0 ± 0.3	16 ± 1	460 ± 6
^{85}Rb	< 0.2	< 0.2	< 0.2	< 0.2	< 0.2	0.7 ± 0.1
^{208}Pb	1.0	0.40 ± 0.03	0.40 ± 0.03	< 0.4	0.50 ± 0.03	0.50 ± 0.03
^{65}Cu	7	<2	<2	<2	2.0 ± 0.5	620 ± 11
^{133}Cs	44	0.30 ± 0.01	0.20 ± 0.01	0.50 ± 0.02	23.30 ± 0.05	760 ± 1
^{138}Ba	9	0.10 ± 0.01	0.20 ± 0.01	1.40 ± 0.04	19.0 ± 0.1	330.0 ± 0.6

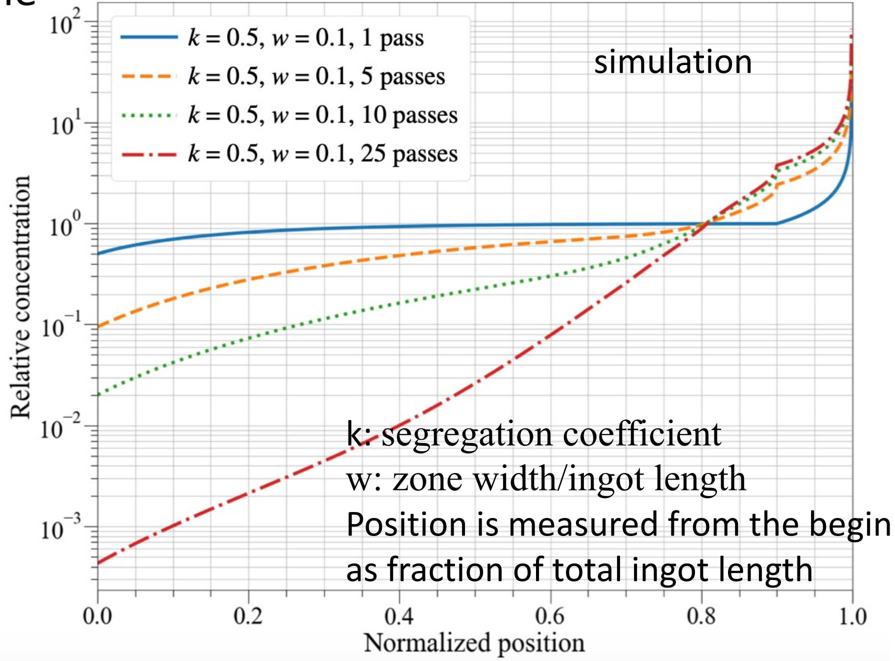

Suerfu B et al . Phys Rev (2021) 16:014060.

Radiogenic background

- Developed some of the lowest background crystals.
- Radiogenic background simulation from NaI-33 measurement.
- The radiogenic background of the crystal in 1 – 6 keV region is mainly due to the contaminants of ^{210}Pb, ^{87}Rb, ^{40}K, ^{238}U…

	^{39}K (ppb)	^{238}U (ppt)	^{210}Pb (mBq/kg)	^{232}Th (ppb)	Active mass (kg)
DAMA [2]	13	0.7-10	(5-30) x 10^{-3}	0.5-7.5	250
ANAIS [3]	31	< 0.81	1.5	0.36	112
COSINE [4]	35.1	< 0.12	1-1.7	<2.4	~60
SABRE (NaI-033) [5]	4.3	0.4	0.49	0.2	~35+40=75 (total goal)
PICOLON [6]	<20	-	< 5.7 x 10^{-3}	-	~20 (goal)

Radiogenic background [1]

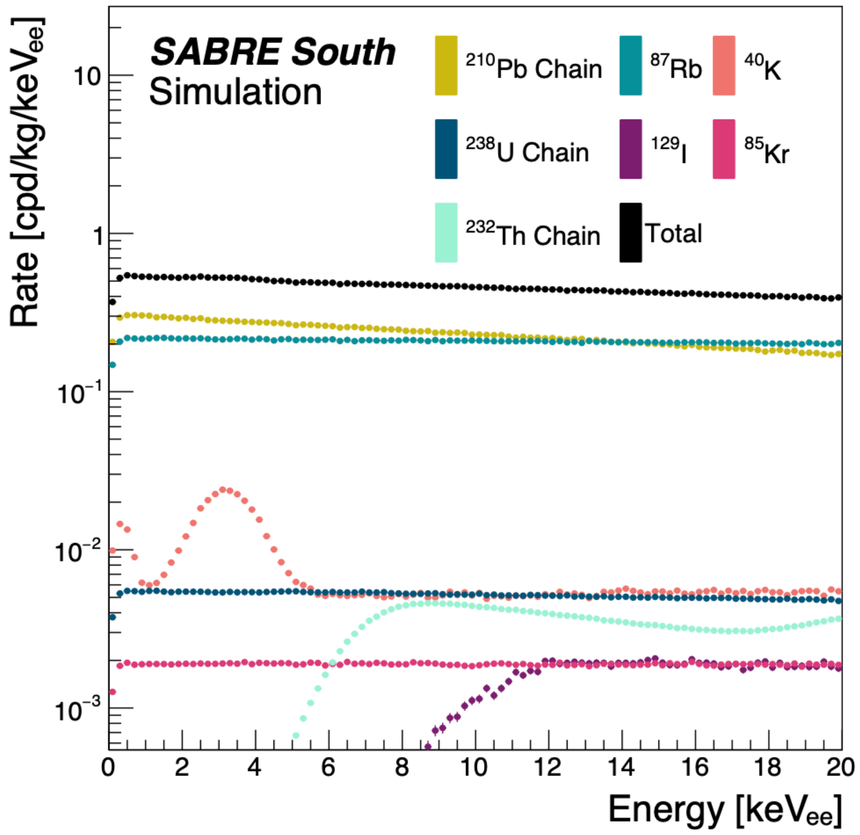

[1] SABRE South, arXiv:2205.13849
[2] DAMA, NIMA 592(3) (2008)
[3] ANAIS, EPJC 79 412(2019)
[4] COSINE, Phys. Rev. Lett. 123, 031302 (2019)
[5] SABRE, EPJC 81, 299 (2021).
[6] PICOLON, PTEP 4 043F01 (2021)

Cosmogenic background

Cosmogenic background of the crystal in 1 – 6 keV region is mostly due to the isotopes produced during transport: ^{3}H, ^{113}Sn, ^{109}Cd, ^{127}Te …
Radiogenic background calculated with ACTIVIA after 6 months cool-down at SUPL.

Cosmogenic background

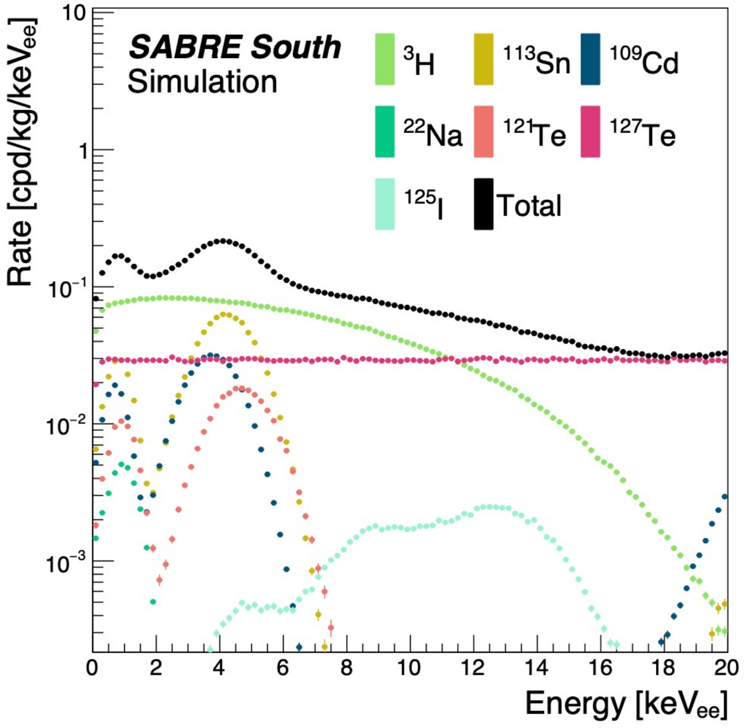

Isotope	Activity[mBq/kg]	Half life [days]
^{3}H	9.4×10^{-3}	4496.8
^{22}Na	4.3×10^{-2}	949.7
^{109}Cd	5.3×10^{-3}	461.4
^{109m}Ag	5.3×10^{-3}	4.6×10^{-4}
^{113}Sn	1.44×10^{-2}	115.1
^{113m}In	1.41×10^{-2}	0.07
^{121m}Te	0.16	164.2
^{121}Te	0.16	19.2
^{123m}Te	8.35×10^{-2}	119.2
^{125m}Te	5.96×10^{-2}	57.4
^{127m}Te	0.14	106.1
^{127}Te	0.14	0.39
^{125}I	0.19	59.4
^{126}I	1.0×10^{-4}	12.9

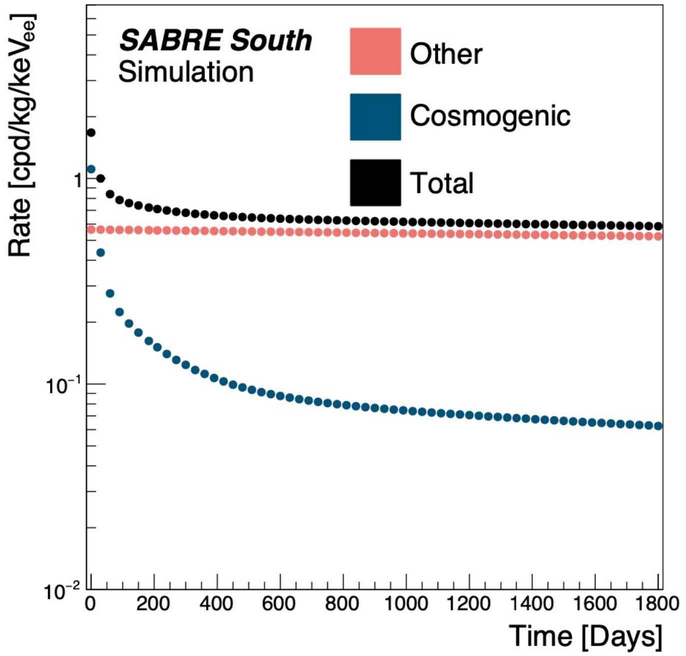

Background rate in the dark matter measurement region as a function of time after first placement underground.

Crystal background

Total background after 6 months cool-down underground.

Total background

Most significant contributions from crystal contamination

Crystal R11065 PMT components:

	[mBq/PMT]		
Isotope	Body	Window	Ceramic plate
^{40}K	< 5.9	< 0.48	6.5
^{60}Co	0.65	< 0.042	< 0.19
^{238}U	< 0.52	< 1.8	13
^{226}Ra	< 0.29	0.040	0.29
^{232}Th	< 0.0098	< 0.037	0.70
^{228}Th	< 0.41	< 0.015	0.13

PTFE reflector:

Isotope	Activity [mBq/kg]
^{40}K	3.1
^{238}U	0.25
^{232}Th	0.5
^{210}pb	3 x 10^{-5}

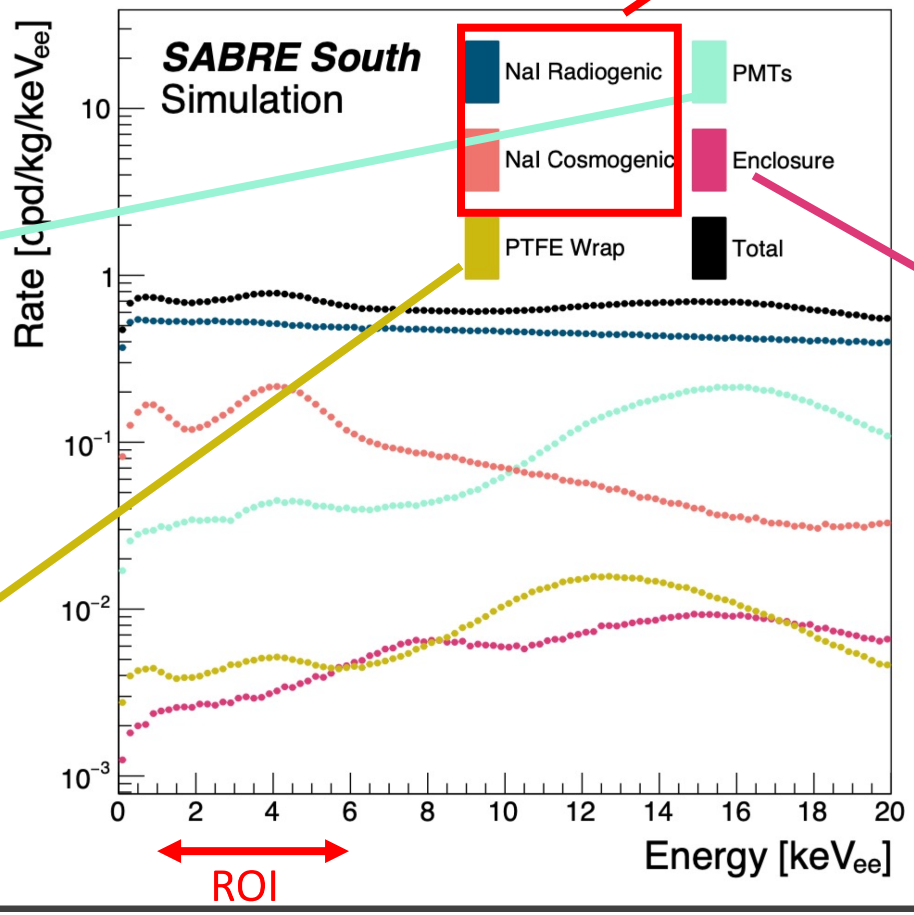

Copper enclosure:

Radiogenic	
Isotope	Activity [mBq/kg]
^{40}K	0.7
^{238}U	0.065
^{232}Th	0.002

Cosmogenic		
Isotope	Activity [mBq/kg]	Half life [days]
^{60}Co	0.340	1925
^{58}Co	0.798	71
^{57}Co	0.519	272
^{56}Co	0.108	77
^{54}Mn	0.154	312
^{46}Sc	0.027	84
^{59}Fe	0.047	44
^{48}V	0.039	16

SABRE Veto

Liquid Scintillator veto system:

- 10 T of linear alkyl benzene (LAB) from JUNO experiment doped with PPO and bis-MSB,
- 18 R5912 veto PMTs;
- Threshold of 50 keV_{ee},
- Veto efficiency for ^{40}K is 87%.

$$veto\ efficiency = \frac{Rate_{veto\ off} - Rate_{veto\ on}}{Rate_{veto\ off}}$$

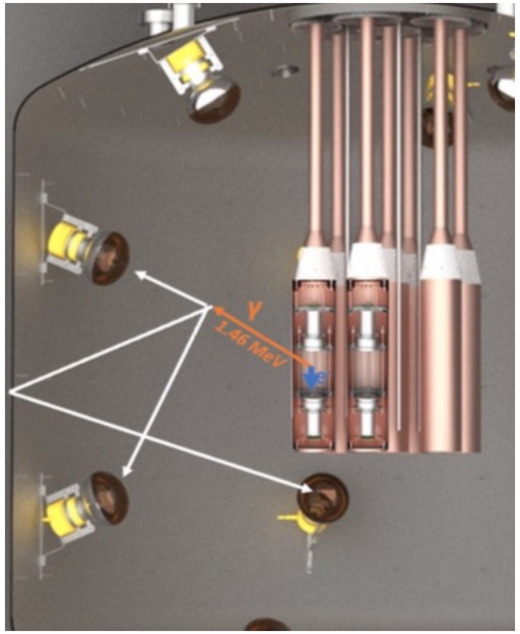

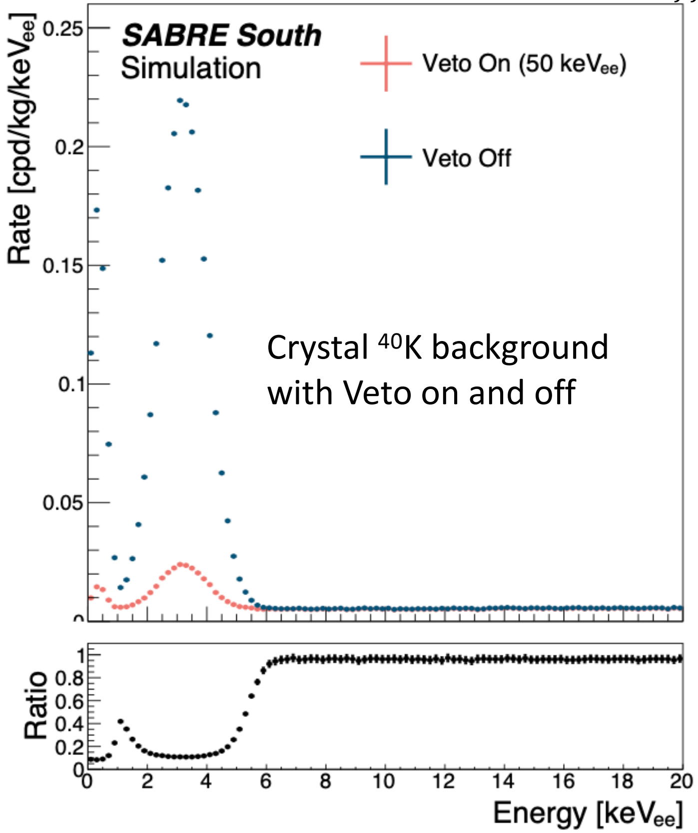

Radiogenic		
Isotope	Rate , veto ON [cpd/kg/keVee]	Rate , veto OFF [cpd/kg/keVee]
^{210}Pb	2.8 x10^{-1}	2.8x10^{-1}
^{87}Rb	< 2.2x10^{-1}	< 2.2x10^{-1}
^{40}K	1.3x10^{-2}	1.0x10^{-1}
^{238}U	< 5.4x10^{-3}	< 5.7x10^{-3}
^{85}Kr	< 1.9x10^{-3}	< 1.9x10^{-3}
^{232}Th	< 3.4x10^{-4}	< 3.9x10^{-4}
^{129}I	9.2x10^{-5}	9.2x10^{-5}
Total	< 5.2x10^{-1}	< 6.0x10^{-1}

Cosmogenic		
Isotope	Rate , veto ON [cpd/kg/keVee]	Rate , veto OFF [cpd/kg/keVee]
^{3}H	7.8x10^{-2}	7.8x10^{-2}
^{113}Sn	3.0x10^{-2}	3.0x10^{-2}
^{121}Te	2.9x10^{-2}	2.9x10^{-2}
^{109}Cd	1.4x10^{-2}	1.4x10^{-2}
^{121}Te	9.1x10^{-3}	1.0x10^{-1}
^{22}Na	5.2x10^{-4}	1.4x10^{-2}
^{125}I	2.3x10^{-4}	2.3x10^{-4}
^{113m}In	7.5x10^{-5}	5.2x10^{-4}
^{127m}Te	4.9x10^{-5}	4.9x10^{-5}
^{126}I	4.1x10^{-5}	6.2x10^{-5}
^{121m}Te	1.8x10^{-5}	6.0x10^{-5}
^{123m}Te	7.3x10^{-6}	1.3x10^{-5}
^{109m}Ag	2.8x10^{-6}	2.8x10^{-6}
^{125m}Te	1.6x10^{-6}	1.7x10^{-6}
Total	1.6x10^{-1}	2.7x10^{-1}

SABRE Veto

- Total background is 0.72 cpd/kg/keV$_{ee}$ (without zone refining), Crystal radiogenic and cosmogenic background contributes ~ 95%.
- Overall veto efficiency of ~27%.

	Rate [cpd/kg/keV$_{ee}$]	Veto Efficiency [%]
Crystal radiogenic	5.2×10^{-1}	13
Crystal cosmogenic	1.6×10^{-1}	40
Crystal PMTs	3.8×10^{-2}	60
PTFE wrap	4.5×10^{-3}	13
Enclosures	3.2×10^{-3}	85
Conduits	1.9×10^{-5}	96
Liquid scintillator	4.9×10^{-8}	> 99
Steel vessel	1.4×10^{-5}	> 99
Veto PMTS	1.9×10^{-5}	> 99
Shielding	3.9×10^{-6}	> 99
External	O(10^{-4})	> 99
Total	7.2×10^{-1}	27

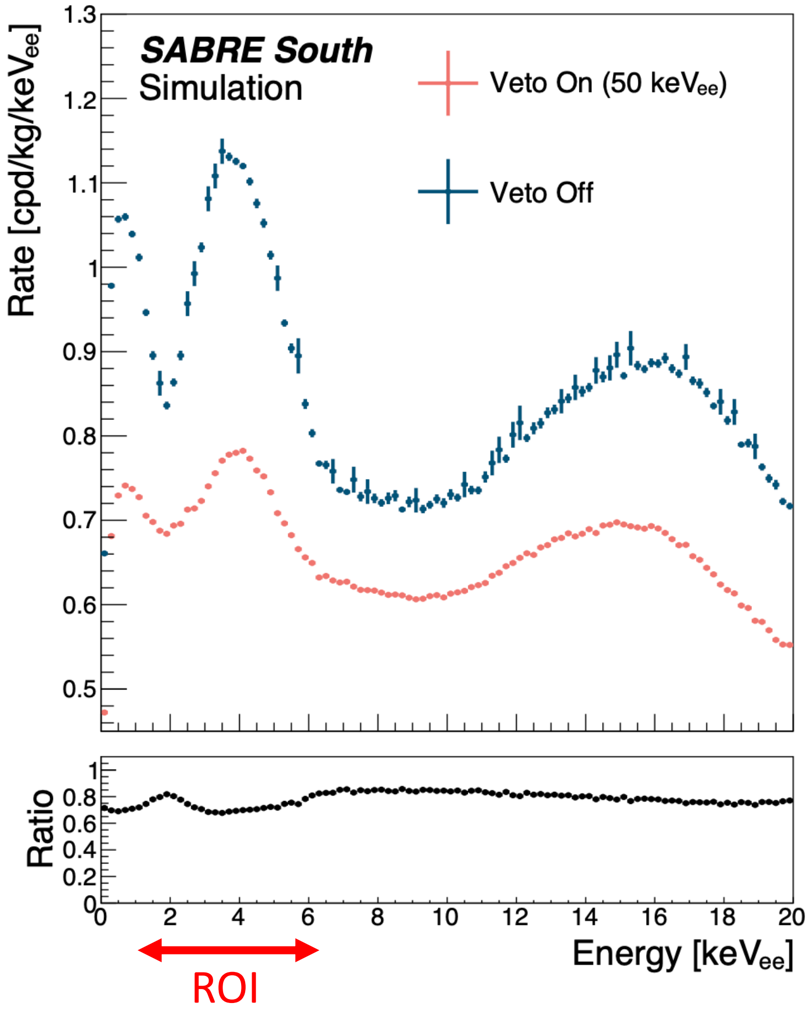

SABRE sensitivity

- With a target mass of 35 kg NaI crystals, and background of 0.72 cpd/kg/keV$_{ee}$ (without zone refining), SABRE South is expected to reach 3σ exclusion and 5σ discovery for the DAMA-like signal after 3 to 5 years of continuous data taking.

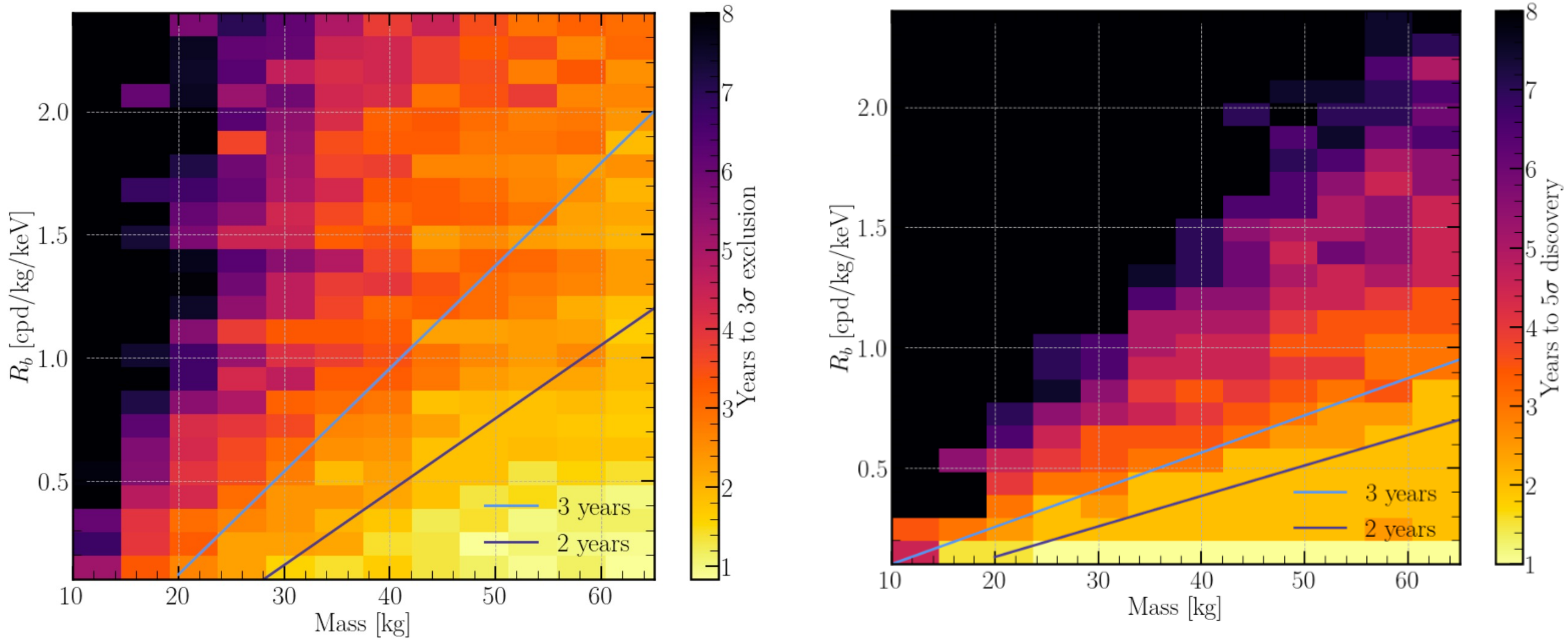

SABRE South Technical Design Report

Crystal PMT characterization

Crystal PMTs are being characterized at the University of Melbourne to understand the response and noise characteristics:

- Dark rate as a function of temperature,
- Single photoelectron response (SPE) & gain,
- Quantum Efficiency (QE),
- Transit time and spread,
- Linearity,
- Afterpulsing.

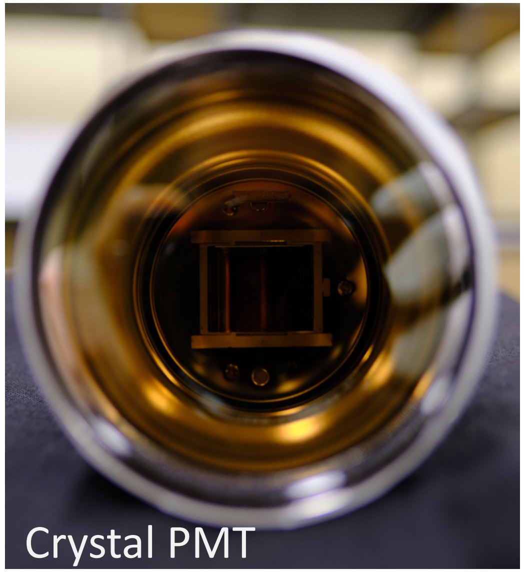

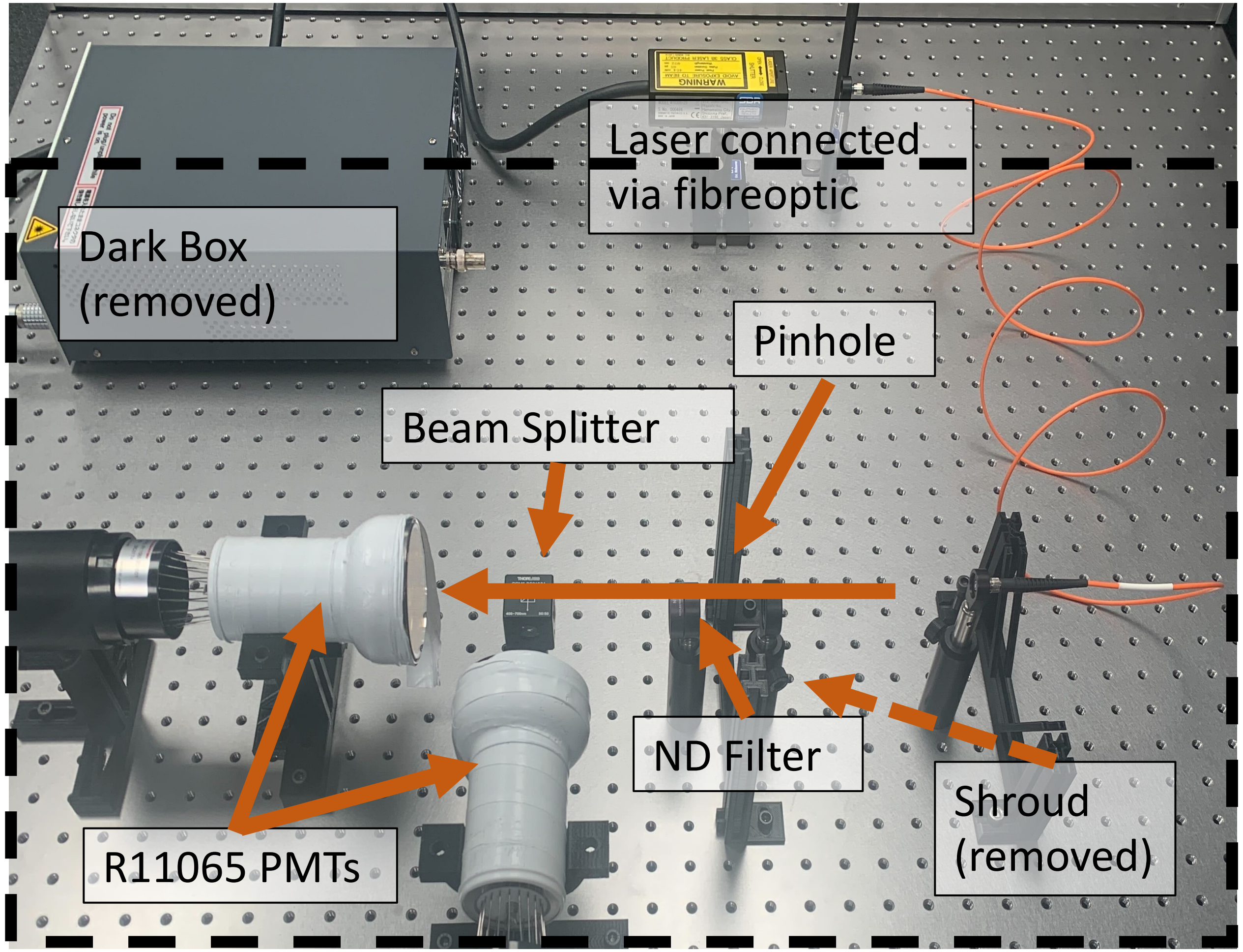

PMT dark rate

Understanding the dependency of PMT noise on temperature and gain

Temperature dependance of dark rate:

$$\mathbf{R} \propto \mathbf{T}^{\frac{5}{4}} * \mathbf{e}^{-q_e \psi / KT}$$

- **T:** Absolute temperature [K]
- **q_e**: Electron charge
- **K**: Boltzmann constant
- **ψ**: Work function

Collect dataset to develop noise classifier

SPE response from thermal noise

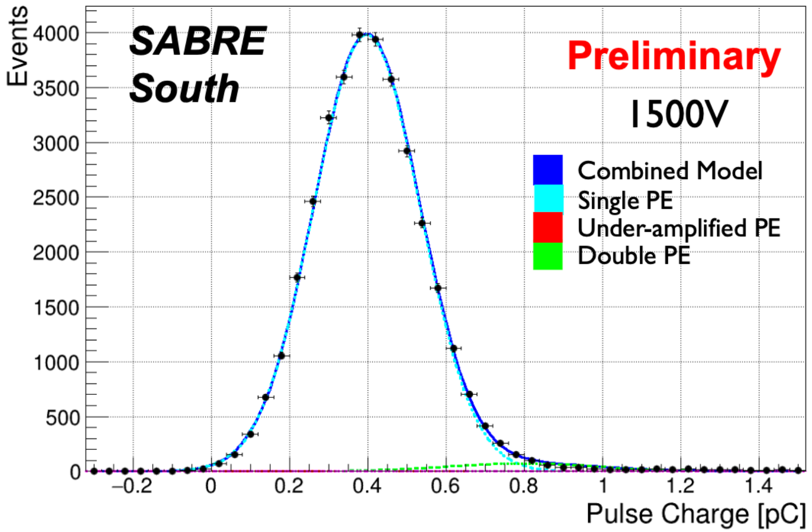

R11065 DR vs Temperature

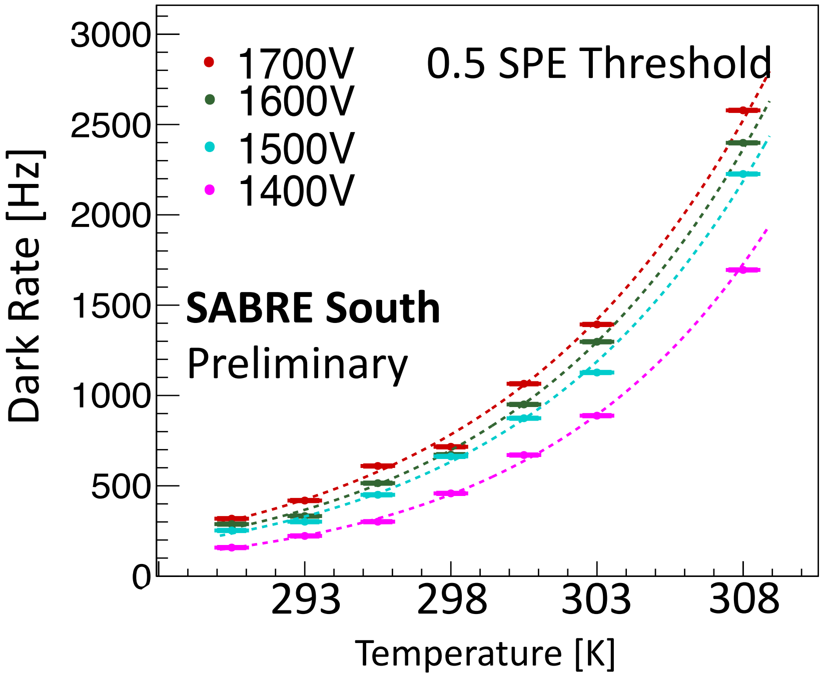

- Gain monitoring from dark rate could allow for constant calibration
- PMT paper is being prepared for publication

PMT SPE

Triggered by pico-second pulsed laser with a mean occupancy of less than 0.05 photons/pulse.
Events in a 20 ns SPE-Region are selected to get a sample of laser triggered events.
R11065 Charge Model

$$\mathbf{PDF} = \sum_{n=1}^{4} \left((1-p)\cdot G(Q_{\mathrm{PE}}, \sigma_{\mathrm{PE}}) + p \cdot G(\delta Q_{\mathrm{PE}}, \delta\sigma_{\mathrm{PE}})\right)^n$$

- $\mathbf{G}(Q_{PE}, \sigma_{PE})$ Gaussian with mean Q_{PE} and sigma σ_{PE}.
- p is a Poissonian probability of under-amplified signal.
- δ is the under-amplified scale parameter.

SPE event selection

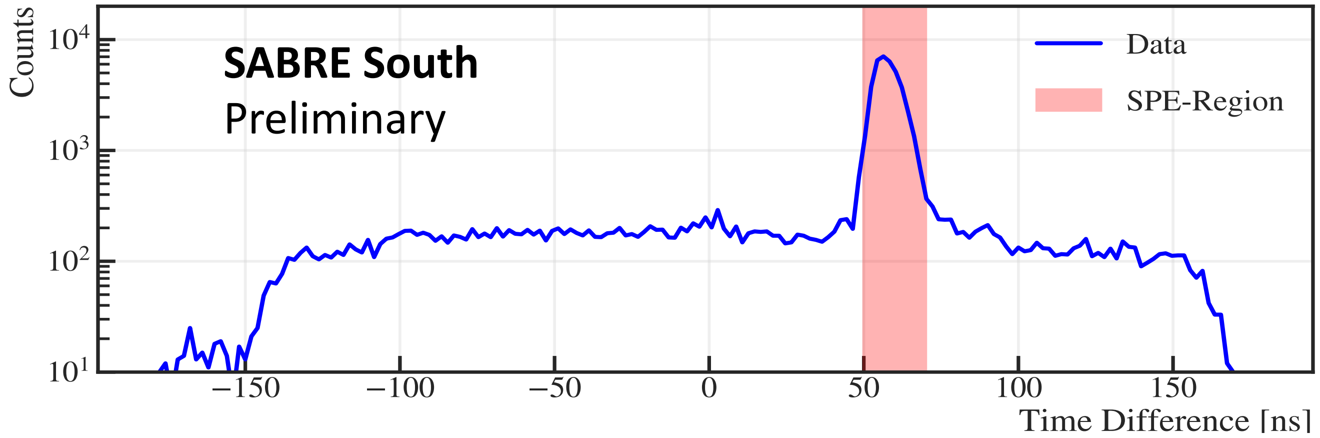

SPE fit

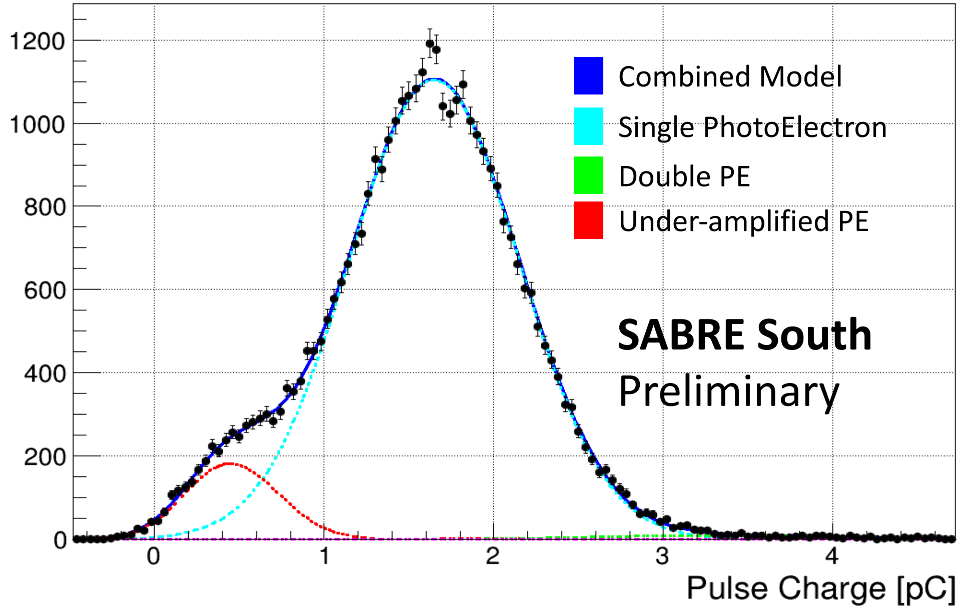

PMT gain

With measured SPE data, the gain can be calculated by: $gain = \frac{Q_{1PE}}{q_e}$;

Consistent with Hamamatsu parameterization: $gain = K * V^{\alpha n}$

- K: constant;
- α: determined by the dynode material and geometry
- n: number of dynode stage

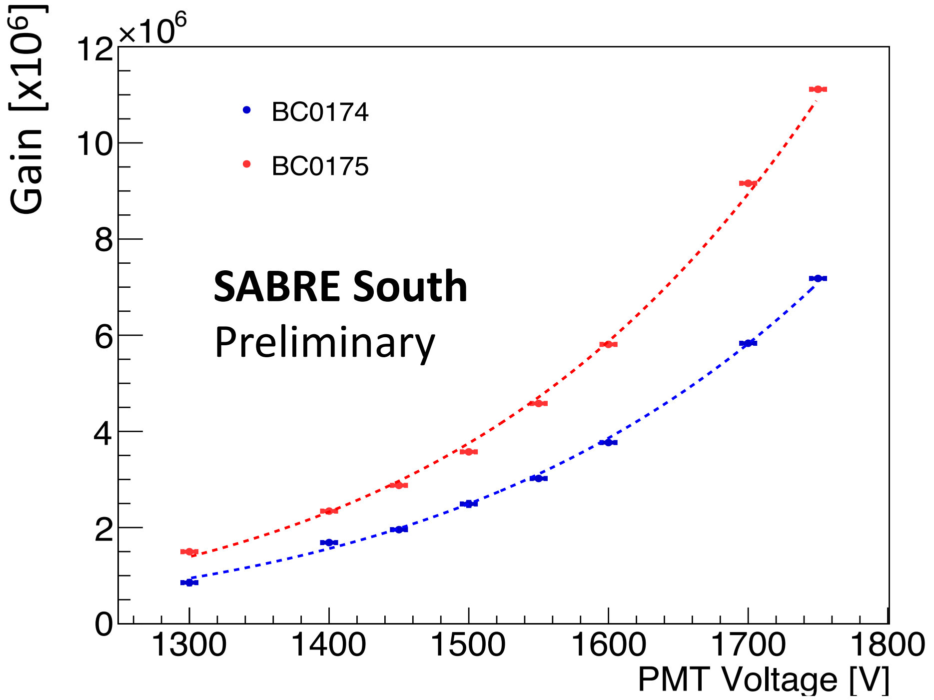

Dark events are used to validate the laser triggered gain measurement. It shows good agreement.

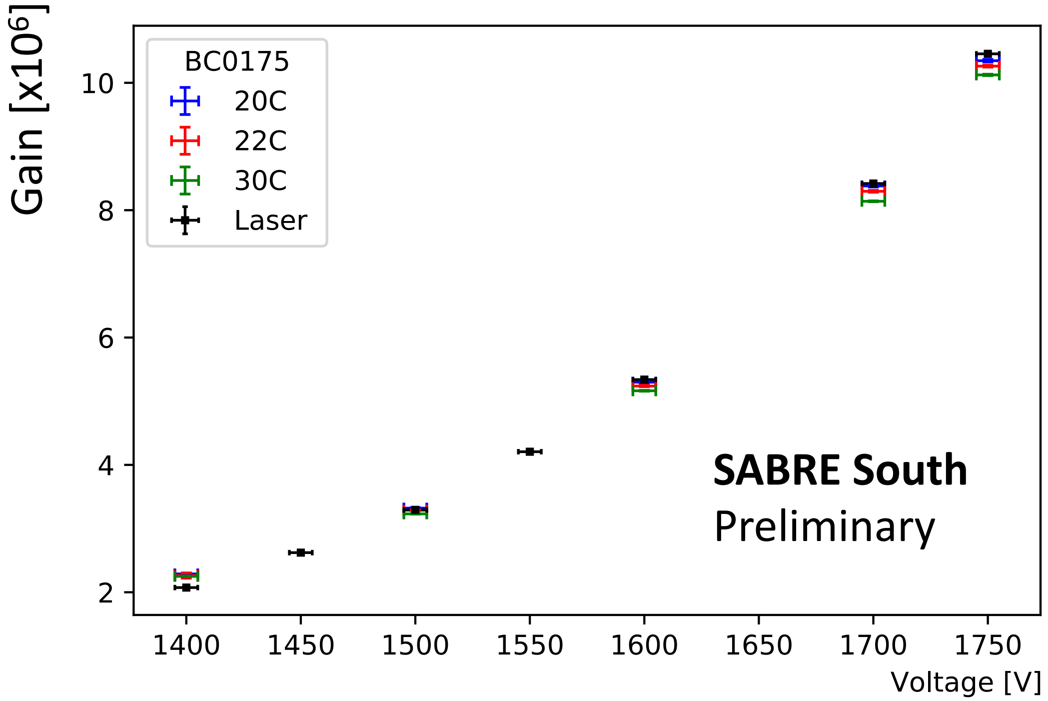

Summary

- SABRE searches for dark matter annual modulation signal with twin detectors located in both hemispheres. Seasonal or site related effects can be disentangled from dark matter modulation.
  - SABRE North at LNGS,
  - SABRE South at SUPL.
- SABRE have developed some of the lowest background crystals.
  - Crystal characterisation is ongoing,
  - Zone refining is going to be used to further reduce the contaminations in ultrahigh-purity powder.
- SABRE South crystal background has been full simulated. The paper has been accepted to EPJC. SABRE South Technical Design Report is online.
- Characterisation of crystal PMTs is ongoing.
- SABRE South commissioning starts from the end of this year and completes in 2024. It is expected to reach 3σ exclusion and 5σ discovery for the DAMA-like signal after 3 to 5 years of continuous data taking.

SABRE North

SABRE South

Backup

SABRE North and South synergy

SABRE North and South detectors have **common core features**:

- Same crystal production and R&D.
- Same detector module concept (Ultra-pure crystals and HPK R11065 PMTs)
- Common simulation, DAQ and data processing frameworks
- Exchange of engineering know-how with official collaboration agreements between the ARC Centre of Excellence for Dark Matter and the INFN

SABRE North and South detectors **have different shielding designs:**

- SABRE North has opted for a fully passive shielding due to the phase out of organic scintillators at LNGS. Direct counting and simulations demonstrate that this is compliant with the background goal of SABRE North at LNGS.
- SABRE South will be the first experiment in SUPL, the liquid scintillator will be used for in-situ evaluation and validation of the background in addition to background rejection and particle identification.

Queching factor

$$E_{ee} = Q(E_{NR})E_{NR}$$

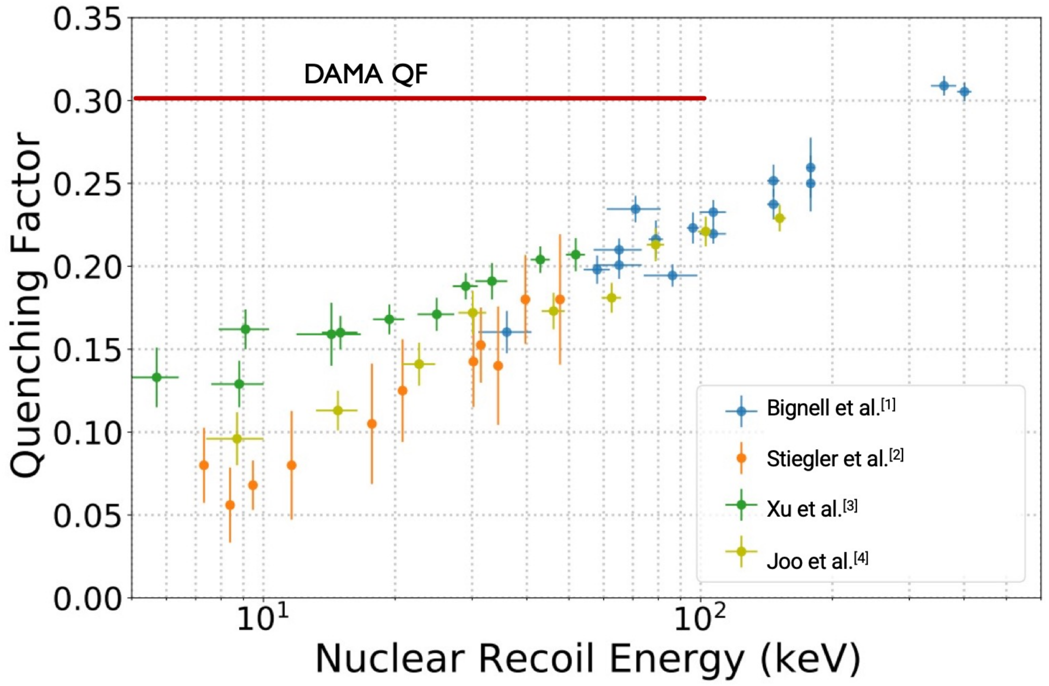

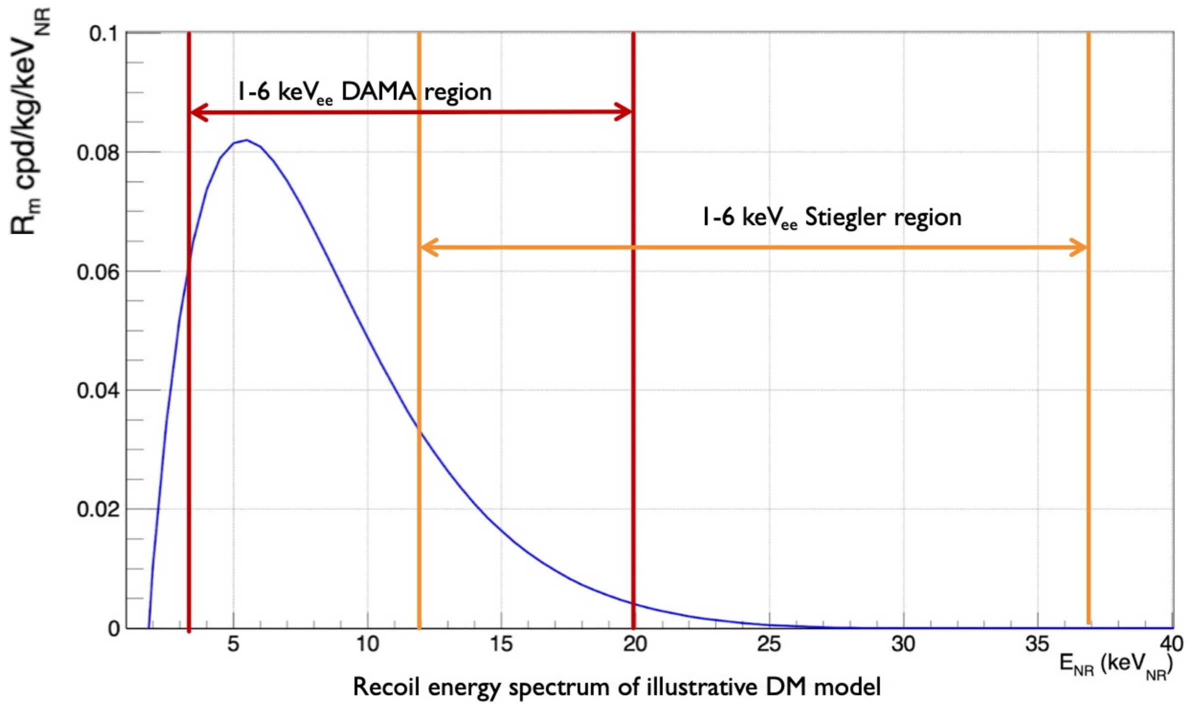

From M. J. ZUROWSKI, IDM, JULY 2022

[1]L.J. Bignell et al 2021 JINST 16 P07034
[2]T. Stiegler et al. 2017 arxiv:1706.07494
[3]J. Xu et al. 2015 10.1103/physrevc.92.015807
[4]H. Joo et al. 2019 10.1016/j.astropartphys.2019.01.001

BG rate of DM experiments

Group	Target	Mass (kg)	BG rate (cpd/kg/keV_{ee})
XENON1T	Xe	1300	2×10^{-4}
LUX	Xe	250	5×10^{-4}
XMASS	Xe	800	4.2×10^{-3}
DAMIC	Si	0.036	15
SuperCDMS	Ge	0.6	2
ANAIS	NaI	112.5	3.2
COSINE - 100	NaI	106	2.7
DAMA / LIBRA	NaI	250	1.0
PICOLON	NaI	1.25	1.5
SABRE	NaI	~35+40=75(total goal)	0.72

arXiv:2106.15235

SABRE South veto

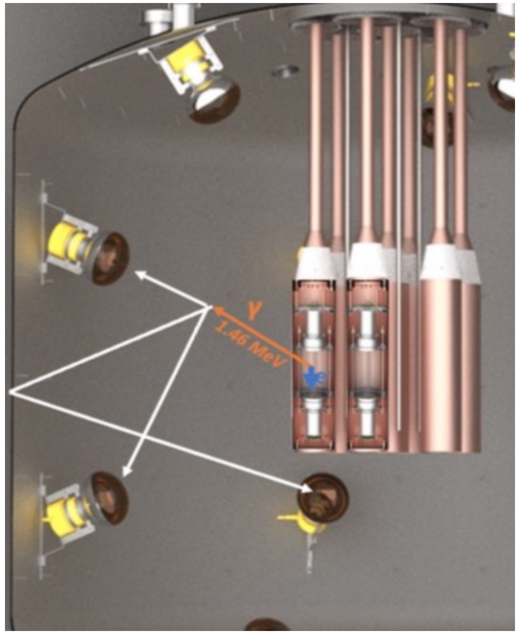

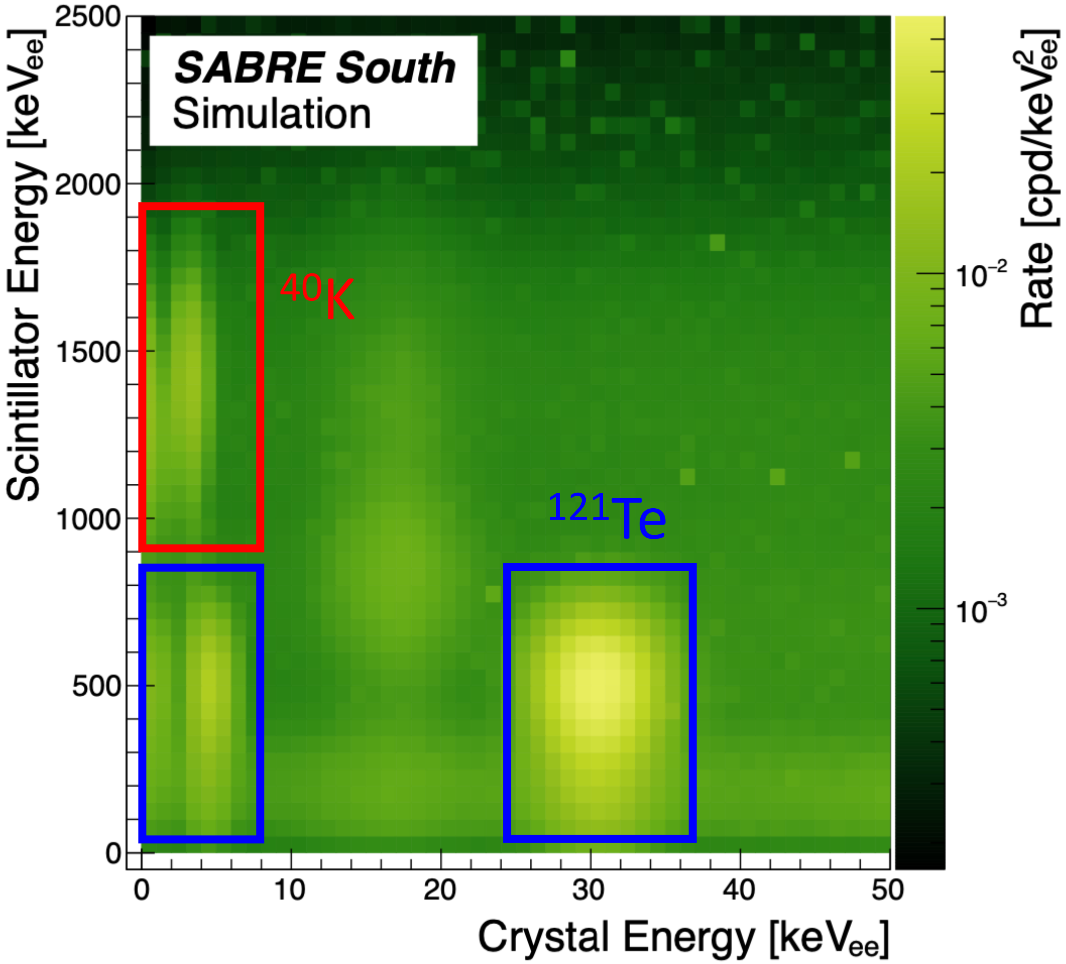

Detector digitisation

Developing software to emulate the detector response for Monte Carlo studies. Recreate response from individual PMTs and DAQ system to produce pseudo data.

Arriving time of photons from Geant4 simulation.

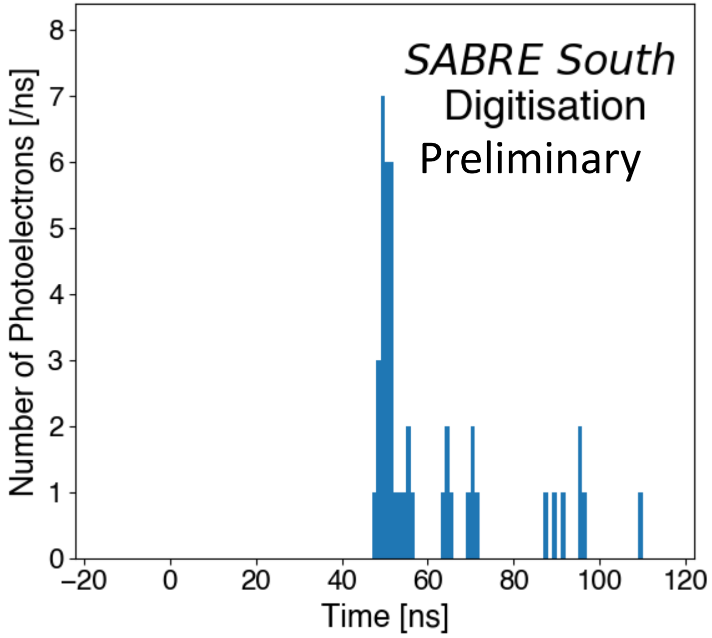

Photon arrival time from MC makes pseudo waveforms

Digitised waveform.